The neural code behind face recognition abilities

Simon Faghel-Soubeyrand[1,2], Meike Ramon[3], Eva Bamps [5], Matteo Zoia [6], Jessica Woodhams [2], Anne-Raphaelle Richoz[4], Roberto Caldara[4], Frédéric Gosselin*[1] & Ian Charest*[1,2]

1. Département de psychologie, Université de Montréal, Canada
2. School of Psychology, University of Birmingham, UK
3. Institute of Psychology, University of Lausanne, Switzerland
4. Département de Psychology, Université de Fribourg, Switzerland
5. Center for Contextual Psychiatry, Department of Neurosciences, KU Leuven, Belgium
6. Department for Biomedical Research, University of Bern, Switzerland

Corresponding authors:
Ian Charest,
i.charest@bham.ac.uk
Simon Faghel-Soubeyrand,
simon.faghel-soubeyrand@umontreal.ca

Word counts. Abstract: 92. Main text : 2292, Method : 4627

Summary

Why are some individuals better at recognising faces? We addressed this question by characterising the brain computations of individuals with extraordinary recognition abilities using high-density electroencephalographic signals and a combination of behavioural tests, artificial neural network models, and machine learning analyses. We found that individual face recognition ability can be decoded from brain activity in an extended temporal interval for face and non-face objects. We show that both visual and semantic brain computations contribute to these individual differences.

Main

The ability to robustly recognise the faces of our colleagues, friends and family members is paramount to our success as social beings. Our brains complete this feat with apparent ease and speed, in a series of computations unfolding within tens of milliseconds in a wide brain network comprising the inferior occipital gyrus, the fusiform gyrus, the superior temporal sulcus, and more anterior areas such as the anterior temporal lobe (Duchaine & Yovel, 2015; Grill-Spector et al., 2017; Kanwisher et al., 1997). Not all individuals, however, are equally competent at recognising faces in their surroundings (White & Burton, 2022). Developmental prosopagnosics show a great difficulty at this task despite an absence of brain injury (Susilo & Duchaine, 2013). In contrast, super-recognisers exhibit remarkable abilities for processing facial identity, who can recognize individuals even after little exposure several years before (Noyes et al., 2017; Ramon, 2021; Russell et al., 2009). The specific nature of the neural processes responsible for these individual differences remains largely unknown. So far, individual differences studies have used univariate techniques to investigate face-specific aspects of brain processing. This revealed that the contrast between responses to faces compared to non-faces, measured by the N170 event-related potential component or by the blood oxygen level dependent signals in regions of interest, are modulated by ability (Elbich & Scherf, 2017; Herzmann et al., 2010; Huang et al., 2014; Kaltwasser et al., 2014; Lohse et al., 2016; Nowparast Rostami et al., 2017; Rossion et al., 2020). However, these univariate techniques are limited in their capacity to reveal the precise nature of the underlying computations (di Oleggio Castello et al., 2021; Dwivedi et al., 2021; Harel et al., 2013). Here, we tackled this challenge with a data-driven approach. We examined the functional differences between the brains of super-recognisers and typical recognisers using decoding and representational similarity analyses (RSA; Kriegeskorte et al. 2008; Kriegeskorte and Kievit 2013; Charest et al. 2014; Dwivedi et al. 2021; Kriegeskorte and Diedrichsen 2019) applied to high-density electrophysiological (EEG) signals and artificial neural network models.

We recruited 33 participants, including 16 super-recognisers, i.e., individuals better than the 98th percentile on a battery of face recognition tests (Russell et al., 2009; **Fig. 1a**). We measured EEG while they performed a one-back task. The objects depicted in the stimuli belonged to multiple visual categories including face images of different sexes, emotions, and identities, as well as images of man-made and non-face natural objects (e.g., a computer, a plant), animals (e.g., a giraffe, a monkey), and scenes (e.g., a city, a dining room; **Fig. 1b**).

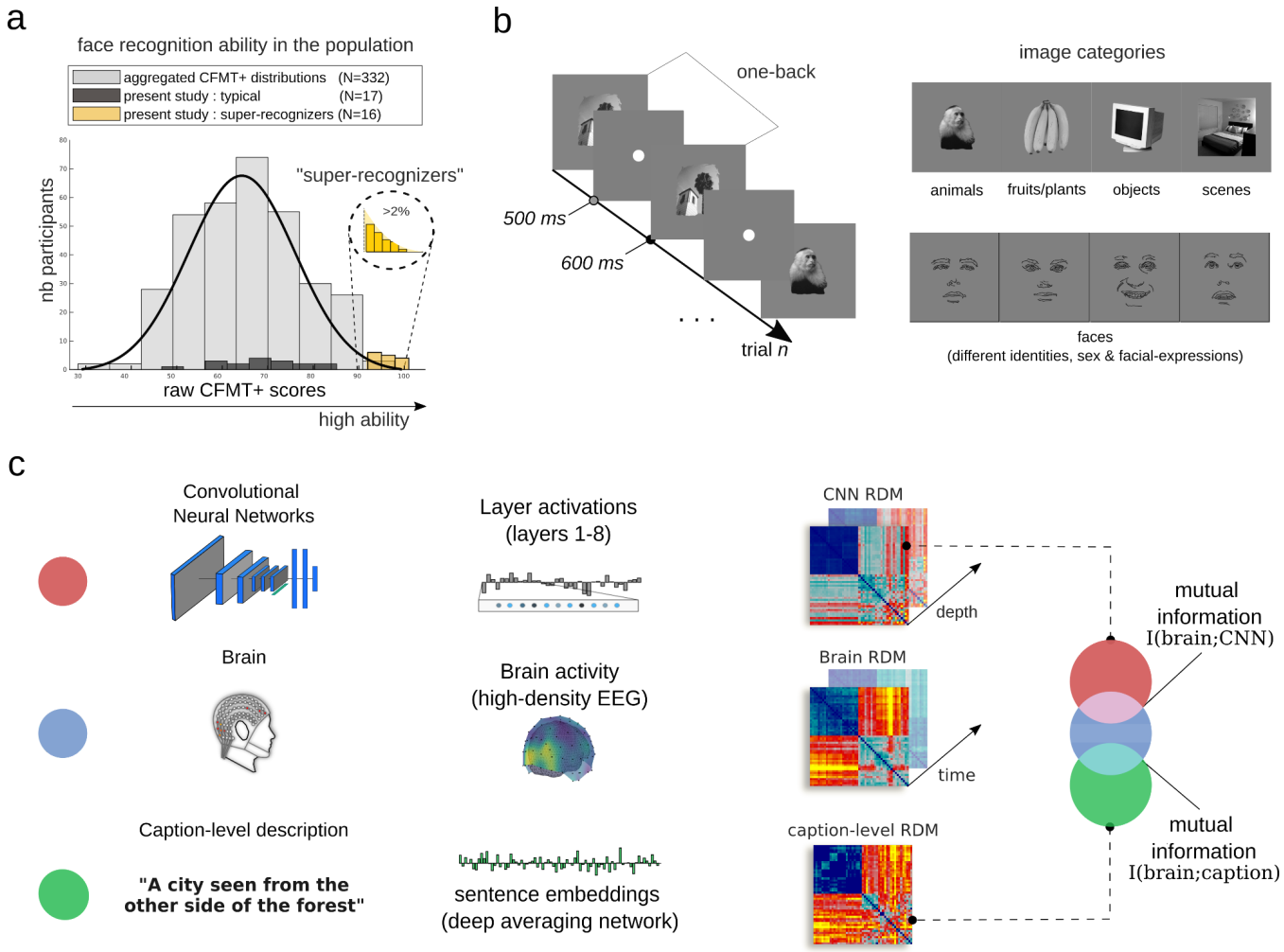

Figure 1. Experimental procedure and computational modelling of brain representations. a) The histogram shows the Cambridge Face Memory Test long-form (CFMT+, Russell et al. 2009) scores of super-recognisers (yellow bars), typical recognisers (black bars), and an additional 332 neurotypical observers from three independent studies for comparison (Faghel-Soubeyrand et al., 2019; Fysh et al., 2020; Tardif et al., 2019). **b)** Participants engaged in a one-back task while their brain activity was recorded with high-density electroencephalography. The objects depicted in the stimuli belonged to various categories, such as faces, objects, and scenes. Note that the face drawings shown here are an anonymised substitute to the experimental face stimuli presented to our participants. **c)** Representational dissimilarity matrices (RDM) were computed from convolutional neural networks (CNN; Krizhevsky et al., 2012; Simonyan & Zisserman, 2014) of vision, human brain activity, and a deep neural network of caption classification and sentence semantics (Cer et al., 2018). To characterise

the CNN RDMs, we computed the pairwise similarity between unit activation patterns for each image independently in each CNN layer. The caption-level RDMs were derived from human caption descriptions of the images transformed into sentence embeddings. Brain RDMs were computed using cross-validated decoding performance between the EEG topographies from each pair of stimuli at every 4 ms time-point. Mutual information (Ince et al., 2017) between the model RDMs and the brain RDMs was assessed, for every participant, at each 4 ms step from stimulus onset.

With this sizable and category-rich dataset, we first attempted to classify a participant as either a super- or a typical recogniser based solely on their brain activity. More specifically, we trained Fisher linear discriminants to predict group membership from single, 1-second trials of EEG patterns (in a moving searchlight of five neighbouring electrodes). We observed up to ~80% cross-validated decoding performance, peaking over electrodes in the right hemisphere. This is all the more impressive given that the noise ceiling imposed on our classification by the test-retest reliability of the CFMT+ (Duchaine and Nakayama 2006; Russell et al. 2009), the gold-standard test used to identify super-recogniser individuals, is a performance of ~93% (SD=2.28%; see Supplementary material). To reveal the time course of these functional differences, we applied the same decoding procedure to each 4-ms interval of EEG recordings. Group-membership predictions attained statistical significance (p<.001, permutation tests, **Fig. 2a**) from about 65 ms to at least 1 s after stimulus onset, peaking around 135 ms, within the N170 window (Bentin et al., 1996; Rossion & Jacques, 2012). Notably, similar results were obtained following the presentation of both face *and* non-face visual stimuli (**Fig. 2a; see also Supplementary Fig. 1**), corroborating a central prediction of domain-general accounts of face recognition (Behrmann & Avidan, 2005; Garrido et al., 2018; Geskin & Behrmann, 2018; Grill-Spector et al., 2004; Kanwisher, 2000).

An ongoing debate in individual differences research is whether the observed effects emerge from qualitative or quantitative changes in the supporting brain mechanisms (Barton & Corrow, 2016; Bobak et al., 2017; Hendel et al., 2019; Maguire et al., 2003; Price & Friston, 2002; Rosenthal et al., 2017; Vogel et al., 2005; Zadelaar et al., 2019). The decoding results presented up to this point might give the impression that face recognition ability is supported by qualitative differences in brain mechanisms. However, these results were obtained with dichotomous classification models applied, by design, to the brains of individuals from a bimodal distribution of ability scores (e.g. Maguire et al., 2003). To better assess the nature of the relationship between brain processing and ability in the general population, we thus performed a new decoding analysis on the typical recognisers only, using a continuous regression model. Specifically, we used cross-validated fractional ridge regression (Rokem & Kay, 2020) to predict *individual* CFMT+ face recognition ability scores from single-trial EEG data. This essentially replicated the previous decoding results: performance was above statistical threshold (p<.01, FDR-corrected) from about 80 ms to at least 1 s, peaking around 135 ms following stimulus onset for both face and non-face stimuli (**Fig. 2b,** peak-rho$_{face}$=.4149 at 133 ms, peak-rho$_{non\text{-}face}$=.4899 at 141 ms). This accurate decoding of individual scores from EEG patterns is compatible with a quantitative account of variations in brain mechanisms

across individuals differing in face recognition abilities. Altogether, our decoding analyses provide evidence for important, quantitative, temporally extended, and domain-general variations in the brain activity supporting face recognition abilities.

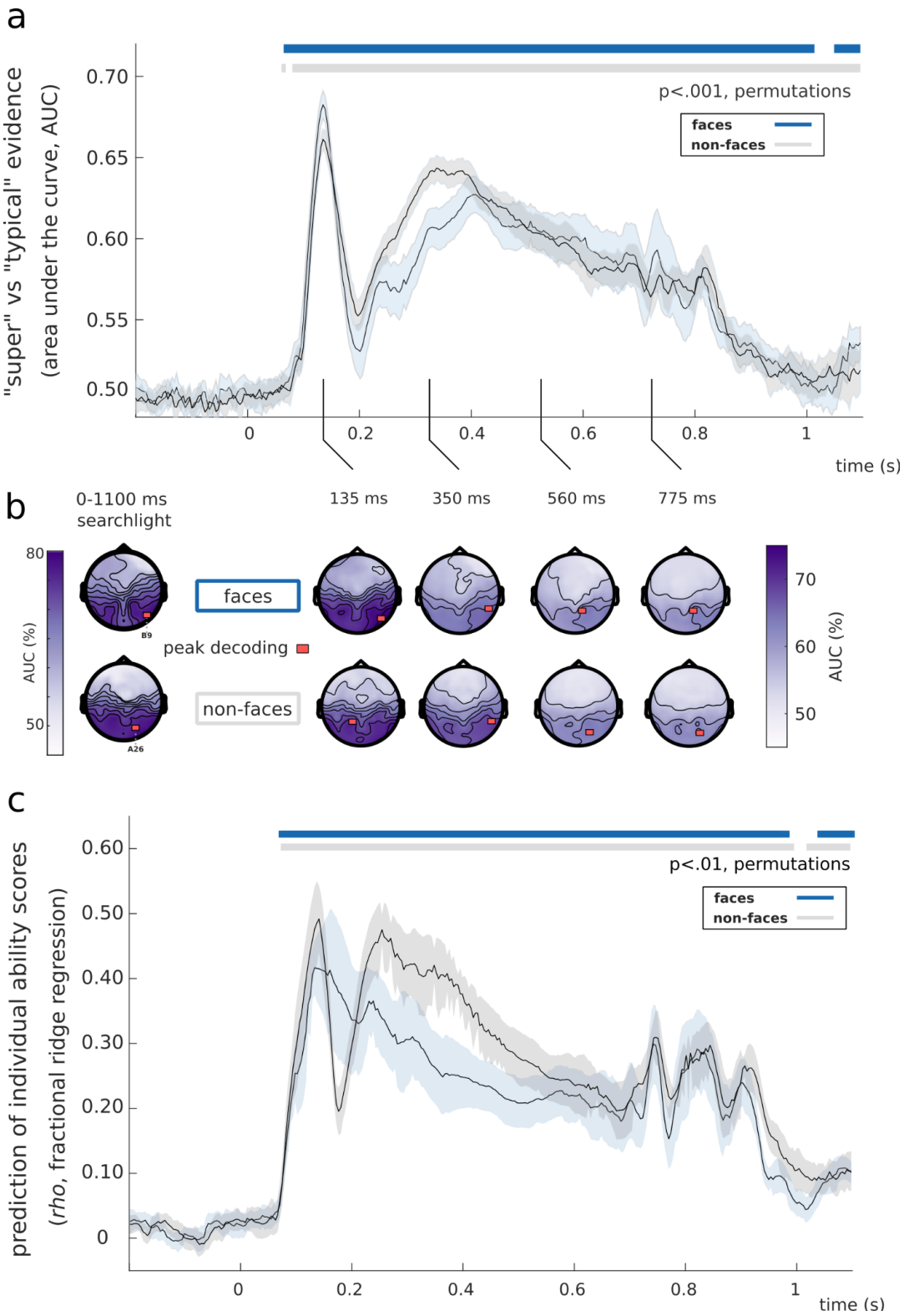

Figure 2. Decoding interindividual recognition ability variations from EEG activity. a) Trial-by-trial group-membership predictions (super-recogniser or typical recogniser) were computed from EEG patterns, for each 4-ms interval, while participants processed face (blue trace) or non-face stimuli (grey trace). Significant decoding performance occurred as early as 65 ms, peaked in the N170 window, and lasted for the remainder of the EEG epochs (p<.001). **b)** Topographies were obtained using searchlight decoding analyses, either concatenating all time points (left topographies) or for selected time-windows (right topographies). Concatenating all time points resulted in peak classification performance of 77.3% over right occipito-temporal electrodes for face and 77.5% over right occipito-temporal electrodes for non-face conditions. In the N170 window, we observed a peak classification performance of 74.8% over right-temporal electrodes for face, and 72.1% over left-temporal electrodes for non-face conditions. **c**) We decoded the CFMT+ scores of the typical recognisers using fractional ridge regression. This yielded similar results with significant decoding as early as 75 ms, peaking around the N170 time window (peak-rho_{face}=.4149, peak-$rho_{non\text{-}face}$=.4899), and lasted for the remainder of the EEG epochs (p<.01, 1K permutations, 10 repetitions).

Decoding time courses, and evidence for domain generality, however, offer limited insights on the level of brain computations (Lamme & Roelfsema, 2000; McDermott et al., 2002). To better characterise the visual brain computations covarying with face recognition ability, we compared, using representational similarity analysis (Kriegeskorte, Mur, & Bandettini, 2008; Kriegeskorte, Mur, Ruff, et al., 2008; Kriegeskorte & Kievit, 8/2013; Charest et al., 2014), the brain representations of our participants to that of convolutional neural networks (CNNs) trained to categorise objects (Krizhevsky et al. 2012; Simonyan and Zisserman 2014; Güçlü and van Gerven 2015). These CNNs process visual features of gradually higher complexity and abstraction along their layers (Güçlü & van Gerven, 2015), from low-level (i.e., orientation, edges) to high-level features (e.g., objects and object parts). The brain representations were characterised by computing representational dissimilarity matrices (RDMs) for each participant and for each 4-ms time interval. These brain RDMs were derived using the cross-validated decoding performance of a linear discriminant model, where brain activity was decoded for every pair of stimuli at a given time interval (Carlson et al., 2013; Cichy et al., 2014; see **Supplementary Fig. 2** for the group-average RDMs and time course of key categorical distinctions). The visual model representations were characterised by computing RDMs from the layers of the CNNs, using Pearson correlations of the unit activations across all pairs of stimuli. Compared to typical participants, we found that the brain RDMs of super-recognisers showed larger mutual information (Ince et al., 2017) with the layer RDMs of CNNs that represent mid-level features (e.g., combinations of edges, contour, shape, texture; Güçlü & van Gerven, 2015; Long et al., 2018) between 133 and 165 ms (**Fig. 3a**, p<.05, cluster-test; see also **Supplementary Fig. 3**).

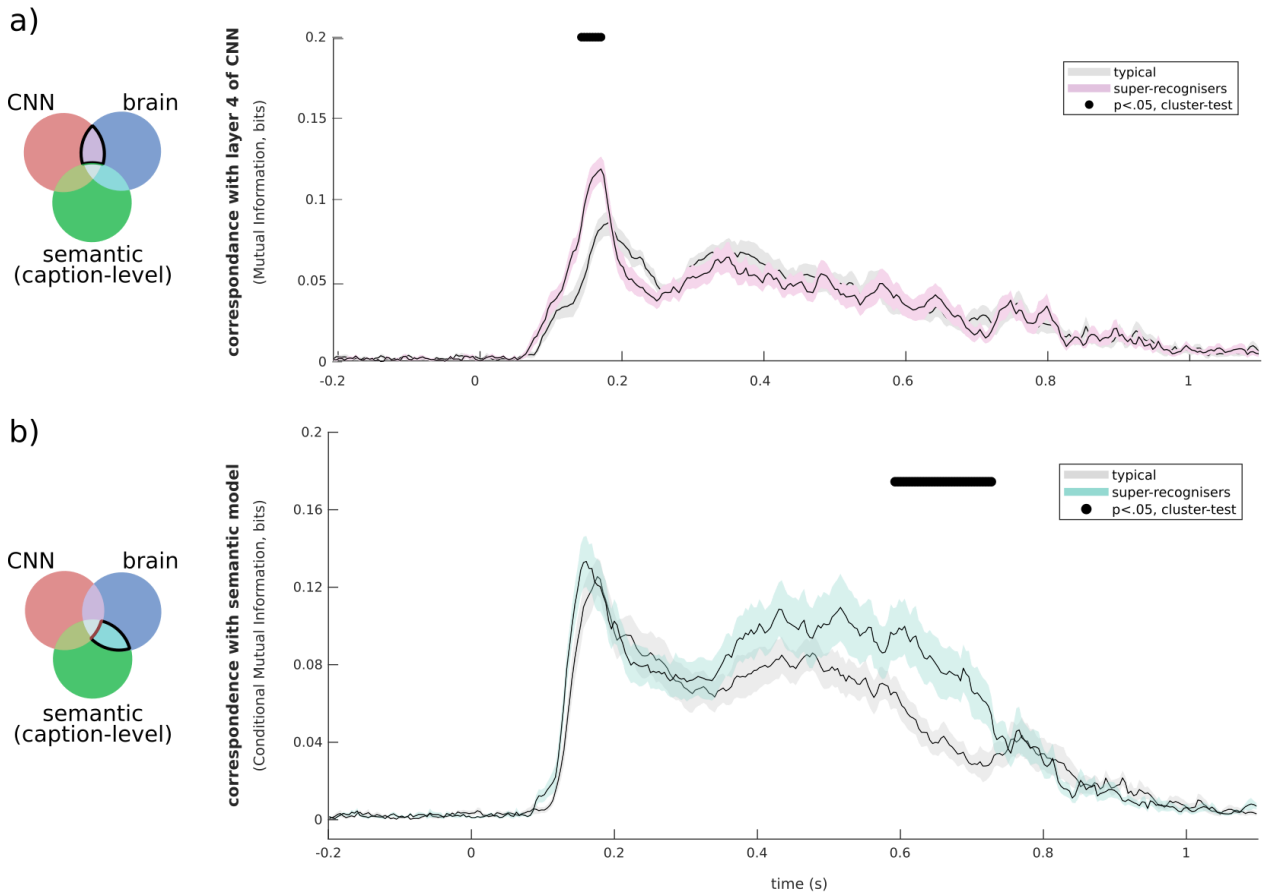

Figure 3. Comparison of super- and typical-recogniser brain representations with those of artificial neural networks of visual and semantic processing. a) Mutual information between brain RDMs and AlexNet RDMs (removing shared mutual information between brain and semantic model) is shown for typical- (grey curve) and super-recognisers (pink curve). We found greater similarity with mid-level visual computations (layer 4 shown, but similar results for layers 3 and 6 and for mid-layers of VGG16, another popular CNN model; see **Supplementary Fig. 3**) in the brains of super-recognisers (black line indicates significant contrasts, p<.05, cluster-corrected) between 133 ms and 165 ms. Similar results were observed when comparing brains and CNN models without removing the shared mutual information between brains and the semantic (caption-level) model (**Supplementary Fig. 3**). **b**) Mutual Information with the semantic model (excluding shared mutual information between brain and AlexNet) differed for typical- and super-recognisers in a later time window centred around 650 ms (cyan curve; super > typical, p < .05, cluster-corrected). Again, similar results were observed when comparing brains and the semantic model without removing the shared mutual information between the brain and AlexNet (**Supplementary Fig. 3**). The shaded areas of all curves represent the standard error.

The finding that decoding was significant as late as 1 s after stimulus onset hints that brain computations beyond what is typically construed as pure visual processing also differ as a function of face recognition ability. To test this hypothesis, we asked five new participants to write captions describing the images presented during our experiment (e.g., “A city seen through a forest.”), and used a deep averaging network (Google Universal Sentence Encoder, GUSE; Cer et al., 2018) to transform these captions into embeddings (points in a caption space). GUSE has been trained to predict semantic textual similarity from human judgments,

and its embeddings generalise to an array of other semantic judgement tasks (Cer et al., 2018). We then compared the RDMs computed from this semantic model to the brain RDMs of both typical- and super-recognisers. Importantly, both this comparison, and the one comparing brain and visual models, excluded the information shared between the semantic and visual models (but see **Supplementary Fig. 3** for similar results with unconstrained analyses). We found larger mutual information with these semantic computations in the brains of super-recognisers than in those of typical recognisers between 598 and 727 ms (**Fig. 3b**, $p<.05$, cluster-test).

Discussion

We investigated the neural mechanisms behind face recognition ability variations using a data-driven approach combining neuroimaging, behavioural tests, and computational models. We recorded the high-density electroencephalographic (EEG) response to face and non-face stimuli in super-recognisers and typical recognisers, and reliably decoded group membership. To characterise the neural computations underlying these group differences, we compared human brain computations with those of artificial neural network models of vision and semantics. This revealed stronger mid-level vision computations early on and stronger semantic computations occurring much later in the brains of super-recognisers compared to those of typical recognisers. To our knowledge, this is the first demonstration of a link between face recognition ability and brain computations beyond high-level vision.

We achieved robust decoding of face recognition ability when examining EEG responses to face *and* non-face stimuli. This domain-general decoding result indicates that mechanisms underlying face recognition abilities give rise to enhanced neural representations that are not restricted to faces. This is consistent with several neuropsychological (Barton et al., 2019; Bobak et al., 2016; Duchaine et al., 2007; Gabay et al., 2017; Geskin & Behrmann, 2018; Hendel et al., 2019) and brain imaging findings (Avidan et al., 2005; Jiahui et al., 2018; Kaltwasser et al., 2014; Rosenthal et al., 2017) showing face and non-face processing effects in individuals across the spectrum of face recognition ability (Behrmann & Plaut, 2013; Harel et al., 2013; but see Duchaine et al., 2006; Furl et al., 2011; Lohse et al., 2016; Wilmer et al., 2012).

The decoding we observed for face and non-face stimuli peaked in the temporal window around the N170 component (Bentin et al., 1996). At that time, the computations in the brains of our participants differed most with respect to the mid-layer computations of artificial models of vision. These layers have been previously linked to processing in human infero-temporal cortex (hIT; Güçlü & van Gerven, 2015; Khaligh-Razavi & Kriegeskorte, 2014) and functionally to mid-level feature representations such as combinations of edges and parts of objects (Güçlü & van Gerven, 2015; Long et al., 2018). This does not mean that the N170 is exclusively involved in these mid-level processes. Rather it suggests that other visual computations,

including the high-level visual computations usually associated with the N170, do not differ substantially between super-recognisers and typical recognisers. The fact that these mid-level features are mostly shared between face and non-face stimuli could explain at least partly the high decoding performance observed for both classes of stimuli.

Finally, we found that face recognition ability is also associated with semantic computations that extend beyond basic-level visual categorisation in a late time-window around the P600 component (Eimer et al., 2012; Shen et al., 2016; van Herten et al., 2005). Recent studies using computational techniques have shown that word representations derived from models of natural language processing explain significant variance in the visual ventral stream (Dwivedi et al., 2021; Fernandino et al., 2022; Popham et al., 2021). The current study goes beyond this recent work in two ways. First, our use of human sentence description and sentence encoders to characterise semantic (caption-level) computations provides a more abstract description of brain representations. Second, and most importantly, our work revealed a link between semantic computations and individual differences in face recognition ability. An association between semantic processes and face recognition ability had been posited in models of face recognition (Bruce & Young, 1986; Duchaine & Yovel, 2015) but, to our knowledge, it had never been shown empirically before.

Methods

Participants

A total of 33 participants were recruited for this study. The first group consisted of 16 individuals with exceptional ability in face recognition — super-recognisers. The second group was composed of 17 neurotypical controls. These sample sizes were chosen according to the effect sizes described in previous multivariate object recognition studies (Carlson et al., 2013; Cichy et al., 2014; Hebart et al., 2018). The data from one super-recogniser was excluded due to faulty EEG recordings. No participant had a history of psychiatric diagnostic or neurological disorder. All had normal or corrected to normal vision. This study was approved by the Ethics and Research Committee of the University of Birmingham, and informed consent was obtained from all participants.

Sixteen previously known super-recognisers were tested in the current study (30-44 years old, 10 female). Eight of these (SR1-SR8) were identified by Prof. Josh Davis from the University of Greenwich using an online test battery comprising a total of six face cognition tasks (Noyes et al., 2021) and tested at the University of Birmingham. The remaining eight (SR-9 to SR-16) were identified using three challenging face cognition tests (Ramon, 2021) and were tested at the University of Fribourg. The behavioural test scores for all participants are provided in **Supplementary Tables 1 and 2.** Across SR cohorts, the Cambridge Face Memory Test long-form (CFMT+; Russell et al., 2009) was used as the measure of face identity processing ability. A score greater than 90 (i.e., 2 SD above average) is typically considered the threshold for super-recognition (Bobak et al., 2016; Davis et al., 2016; Russell et al., 2009). Our 16 super-recognisers all scored above 92 (M=95.31; SD=2.68). A score of 92 corresponds to the 99th percentile according to our estimation from a group of 332 participants from the general

population recruited in three independent studies (Faghel-Soubeyrand et al., 2019; Fysh et al., 2020; Tardif et al., 2019).

An additional 17 typical recognisers (20-37 years old, 11 female) were recruited and tested on campus at the University of Fribourg (n=10) and the University of Birmingham (n=7). Their CFMT+ scores ranged from 50 to 85 (M=70.00; SD=9.08). Neither the average nor the distribution of this sample differed significantly from those of the 332 participants from the general population mentioned above (see **Fig. 1a**; t(346)=1.3065, *p*=0.1922; two-sample Kolmogorov-Smirnov test; D(346)=0.2545, *p*=0.2372).

Tasks

CFMT+

All participants were administered the CFMT long-form, or CFMT+ (Russell et al., 2009). In the CFMT+, participants are required to memorise a series of face identities, and to subsequently identify the newly learned faces among three faces. It includes a total of 102 trials of increasing difficulty. The duration of this test is about 15 minutes. EEG was not recorded while participants completed this test.

One-back task

Stimuli. The stimuli used in this study consisted of 49 images of faces, animals (e.g., giraffe, monkey, puppy), plants, objects (e.g., car, computer monitor, flower, banana), and scenes (e.g., city landscape, kitchen, bedroom). The 24 faces (13 identities, 8 males, and 8 neutral, 8 happy, 8 fearful expressions) were sampled from the Radboud Face dataset (Langner et al., 2010). The main facial features were aligned across faces using Procrustes transformations. Each face image was revealed through an ellipsoid mask that excluded non-facial cues. The non-face images were sampled from the stimulus set of Kiani et al. (Kiani et al., 2007). All stimuli were converted to 250 x 250 pixels (8x8 deg of visual angle) greyscale images. The mean luminance and the luminance standard deviation of these stimuli were equalised using the SHINE toolbox (Willenbockel et al., 2010).

Procedure. We measured high-density electroencephalographic (EEG; sampling rate = 1024 Hz; 128-channel BioSemi ActiveTwo headset) activity while participants performed ~3200 trials of a one-back task in two recording sessions separated by at least one day and by a maximum of two weeks (**Fig. 1b**). Participants were asked to press a computer keyboard key on trials where the current image was identical to the previous one. Repetitions occurred with a 0.1 probability. They were asked to respond as quickly and accurately as possible. Feedback about accuracy was given on each trial. A trial unravelled as follows: a white fixation point was presented on a grey background for 500 ms (with a jitter of ± 50 ms); followed by a stimulus presented on a grey background for 600 ms; and, finally, by a white fixation point on a grey background for 500 ms. Participants had a maximum of 1100 ms following stimulus onset to respond. This interval, as well as the 200 ms preceding stimulus onset, constituted the epoch selected for our EEG analyses.

Analyses

All reported analyses were performed independently for each EEG recording session and then averaged. Analysis were completed using custom code written in MATLAB (MathWorks) and Python.

EEG preprocessing

EEG data was preprocessed using FieldTrip (Oostenveld et al., 2011): continuous raw data was first re-referenced relative to Cz, filtered with a band-pass filter [0.01-80 Hz], segmented into trial epochs from -200 ms to 1100 ms relative to stimulus onset, and down-sampled at 256 Hz.

Decoding analyses

Whole-brain analyses. To predict group-membership from EEG brain activity, we trained Fisher linear discriminant classifiers (5-fold cross-validation, 5 repetitions; Treder, 2020), using all 128 channels single-trial EEG data as features. Separate analyses were done on either all time points after stimulus onset, or successive 4-ms EEG time intervals. The classifiers were trained on trials of EEG activity of participants viewing faces and non-faces independently. The Area Under the Curve (AUC) was used to assess sensitivity. Additional control decoding analyses investigating effects of one-back trials on the predictions are shown in **Supplementary Fig. 1.**

Searchlight analysis. We conducted a searchlight analysis decoding EEG signals from all subsets of five neighbouring channels to characterise the scalp topographies of group-membership AUC. This searchlight analysis was done either using the entire EEG time series of a trial (0-1100 ms; **Fig. 2b,** leftmost topographies), or using 60 ms temporal windows (centred on 135 ms, 350 ms, 560 ms, and 775 ms; **Fig. 2b** rightmost topographies). We ran additional control searchlight decoding procedures investigating the effect of one-back trials (**Supplementary Fig. 1**).

Regression analysis. We used fractional ridge regression models (Rokem & Kay, 2020) to predict individual face recognition ability scores (CFMT+) among the typical recognisers from EEG patterns across time. We trained our model on subsets of 60% of the EEG patterns. We chose the alpha hyperparameter with the best coefficient of determination among 20 alpha hyperparameters ranging linearly from 0.001 to 0.99 applied on a 30% validation set. The decoding performance was assessed using the Spearman correlation between the CFMT+ scores and predictions from the overall best model (applied on the remaining 10% of EEG patterns). This process was repeated 10 times and the Spearman correlations were averaged. Significance was assessed using a permutation test (see *Group comparisons and inferential statistics* section).

Representational Similarity Analysis of brain and computational models

We compared our participants' brain representations to those from visual and semantic (caption-level) artificial neural networks using Representational Similarity Analysis (RSA; Charest et al., 2014; Kriegeskorte, Mur, & Bandettini, 2008; Kriegeskorte, Mur, Ruff, et al., 2008; Kriegeskorte & Kievit, 8/2013).

Brain Representational Dissimilarity Matrices. For every participant, we trained a Fisher linear discriminant to distinguish pairs of stimuli from every 4-ms intervals of EEG response (on all 128 channels) to these stimuli from -200 to 1100 ms after stimulus onset (Cichy & Oliva, 2020; Graumann et al., 2022). Cross-validated AUC served as pairwise classification dissimilarity metric. By repeating this process for all possible pairs (1176 for our 49 stimuli), we obtained a representational dissimilarity matrix (RDM). RDMs are shown for selected time points in **Supplementary Fig. 2**.

Visual Convolutional Neural Networks RDMs*.* We used a pre-trained AlexNet (Krizhevsky et al., 2012) as one model of the visual computations along the ventral stream (Güçlü & van Gerven, 2015). Our 49 stimuli were input to AlexNet. Layer-wise RDMs were constructed comparing the unit activation patterns for each pair of images using Pearson correlations. Similarly, we computed layer-wise RDMs from another well-known CNN, VGG-16 (see **Supplementary Fig. 3b**). Following previous studies using this model (Liu et al. 2021; Xie et al. 2020), we averaged the convolutional layer RDMs situated between each max pooling layers and the layers' input into five aggregated convolutional RDMs (e.g. conv1-1 & conv1-2 into RDM-conv1); this facilitated the comparison of our results with the five convolutional layers of AlexNet.

Semantic Caption-level Deep Averaging Neural Network RDM*.* We asked five new participants to provide a sentence caption describing each stimulus (e.g., "a city seen from the other side of the forest", see **Fig. 1d**) using the Meadows online platform (www.meadows-research.com). The sentence captions were input in Google's universal sentence encoder (GUSE; Cer et al., 2018) resulting in 512 dimensional sentence embeddings for each stimulus. We then computed the dissimilarities (cosine distances) between the sentence embeddings across all pairs of captions, resulting in a semantic caption-level RDM for each participant. The average RDM was used for further analyses.

Comparing brain representations with computational models

We compared our participants' brain RDMs to those from the vision (Fig. 3a) and semantic (Fig. 3b) models described in the previous section using Conditional Mutual Information (CMI, Ince et al., 2017), which measures the statistical dependence between two variables (e.g. mutual information $I(x;y)$), removing the effect from a third variable (i.e. $I(x;y|z)$). Additional control comparisons using unconstrained Mutual Information between brain RDMs and both models are shown in **Supplementary Fig. 3a.**

Group comparison and inferential statistics

Comparison of Conditional Mutual Information time courses. Time courses of CMI were compared between the super-recognisers and typical recognisers using independent samples

t-tests and a Monte Carlo procedure at a *p-value* of .05, as implemented in the Fieldtrip Toolbox (Oostenveld et al., 2011). Family-wise errors were controlled for using cluster-based corrections, with maximum cluster size as cluster-level statistic and an arbitrary *t* threshold for cluster statistic of [-1.90, 1.90] for the comparison of brain and semantic (excluding CNN) and [-2.75 2.75] for the comparison of brain and CNN (excluding semantic) time courses. The standard error is shown for all curves as colour-shaded areas (**Fig. 3**). Analyses with MI (brain; CNN) and MI (brain; semantic) were completed in an identical manner (**Supplementary Fig. 3**).

Time course of group-membership decoding. Significance was assessed using non-parametric permutation tests. We simulated the null hypothesis by training the linear classifier to identify shuffled group-membership labels from the experimental EEG patterns. This process was repeated 1000 times for each time point and each one of the two sessions. We then compared the real, experimental decoding value at each time point to its corresponding null distribution, and rejected the null hypothesis if the decoding value was greater than the prescribed critical value at a p <.001 level.

Time course of individual ability decoding using ridge regression. Significance was again assessed using non-parametric permutation testing. The ridge regression analysis predicted cross-validated CFMT+ scores from single trial EEG patterns, and goodness of fit is reported using Spearman's correlation between the predicted and observed CFMT+ scores. Under the null hypothesis that all participants elicited comparable EEG response patterns, irrespective of their CFMT+ score, the face recognition ability scores are exchangeable. We simulated this null hypothesis by repeating the ridge regression model training using randomly shuffled CFMT+ scores. The predicted CFMT+ scores were then correlated to the empirical, observed CFMT+ scores using Spearman's correlation, and this was repeated 1000 times for each time point. We finally compared the real, experimental correlation value with its corresponding null distribution at each time point, and rejected the null hypothesis if the correlation value was greater than the prescribed critical value at a p <.01 level.

Data availability

Data associated with this article will be available online upon publication of the manuscript.

Code availability

The MATLAB and Python codes used in this study will be available online upon publication of the manuscript.

Acknowledgements

We thank Prof. Josh P. Davis for sharing behavioural scores of super-recognisers and establishing first contact to the UK-based Super-Recognizers reported here. Funding for this project was supported by an ERC Starting Grant [ERC-StG-759432] to I.C, an ERSC-IAA grant to J.W., I.C. and S.F.S., by a Swiss National Science Foundation PRIMA (Promoting Women in

Academia) grant [PR00P1_179872] to MR, and by NSERC and IVADO graduate scholarships to S.F.S. We also thank Mick Neville, from Super-Recognisers Ltd., who helped us to get in contact with some of our super-recognizer participants.

Author contributions
(CRediT standardised author statement)

S.F-S.: Conceptualisation, methodology, software, formal analysis, investigation, data curation, writing - original draft, visualisation, supervision, project administration, funding acquisition. **M.R.:** Investigation, resources, project administration, writing - review and editing. **E.B.:** investigation, project administration. **M.Z.**: investigation. **J.W.:** funding acquisition, writing - review and editing. **A-R.R.**: Investigation. **R.C.:** Resources. **F.G.:** Methodology, writing - original draft, supervision, funding acquisition. **I.C.**: Supervision, methodology, software, resources, formal analysis, writing - original draft, project administration, funding acquisition.

Competing interests

The authors declare no competing interests.

References

Arrington, M., Elbich, D., Dai, J., Duchaine, B., & Suzanne Scherf, K. (2022). Introducing the female Cambridge face memory test – long form (F-CFMT). In *Behavior Research Methods*. https://doi.org/10.3758/s13428-022-01805-8

Avidan, G., Hasson, U., Malach, R., & Behrmann, M. (2005). Detailed Exploration of Face-related Processing in Congenital Prosopagnosia: 2. Functional Neuroimaging Findings. In *Journal of Cognitive Neuroscience* (Vol. 17, Issue 7, pp. 1150–1167). https://doi.org/10.1162/0898929054475145

Barton, J. J. S., Albonico, A., Susilo, T., Duchaine, B., & Corrow, S. L. (2019). Object recognition in acquired and developmental prosopagnosia. In *Cognitive Neuropsychology* (Vol. 36, Issues 1-2, pp. 54–84). https://doi.org/10.1080/02643294.2019.1593821

Barton, J. J. S., & Corrow, S. L. (2016). The problem of being bad at faces. *Neuropsychologia*, *89*, 119–124. https://doi.org/10.1016/j.neuropsychologia.2016.06.008

Behrmann, M., & Avidan, G. (2005). Congenital prosopagnosia: face-blind from birth. *Trends in Cognitive Sciences*, *9*(4), 180–187. https://doi.org/10.1016/j.tics.2005.02.011

Behrmann, M., & Plaut, D. C. (2013). Distributed circuits, not circumscribed centers, mediate visual recognition. *Trends in Cognitive Sciences*, *17*(5), 210–219. https://doi.org/10.1016/j.tics.2013.03.007

Bentin, S., Allison, T., Puce, A., Perez, E., & McCarthy, G. (1996). Electrophysiological studies of face perception in humans. *Journal of Cognitive Neuroscience*, *8*. https://doi.org/10.1162/jocn.1996.8.6.551

Bobak, A. K., Bennetts, R. J., Parris, B. A., Jansari, A., & Bate, S. (2016). An in-depth cognitive examination of individuals with superior face recognition skills. In *Cortex* (Vol. 82, pp. 48–62). https://doi.org/10.1016/j.cortex.2016.05.003

Bobak, A. K., Parris, B. A., Gregory, N. J., Bennetts, R. J., & Bate, S. (2017). Eye-Movement Strategies in Developmental Prosopagnosia and “Super” Face Recognition. In *Quarterly Journal of Experimental Psychology* (Vol. 70, Issue 2, pp. 201–217). https://doi.org/10.1080/17470218.2016.1161059

Bruce, V., & Young, A. (1986). Understanding face recognition. *British Journal of Psychology* , *77 (Pt 3)*, 305–327. https://doi.org/10.1111/j.2044-8295.1986.tb02199.x

Carlson, T. A., Tovar, D. A., Alink, A., & Kriegeskorte, N. (2013). Representational dynamics of object vision: The first 1000 ms. *Journal of Vision*, *13*(10), 1–1. https://doi.org/10.1167/13.10.1

Cer, D., Yang, Y., Kong, S.-Y., Hua, N., Limtiaco, N., St. John, R., Constant, N., Guajardo-Cespedes, M., Yuan, S., Tar, C., Sung, Y.-H., Strope, B., & Kurzweil, R. (2018). Universal Sentence Encoder. In *arXiv [cs.CL]*. arXiv. http://arxiv.org/abs/1803.11175

Charest, I., Kievit, R. A., Schmitz, T. W., Deca, D., & Kriegeskorte, N. (2014). Unique semantic

space in the brain of each beholder predicts perceived similarity. *Proceedings of the National Academy of Sciences*, *111*(40), 14565–14570.

Cichy, R. M., & Oliva, A. (2020). A M/EEG-fMRI Fusion Primer: Resolving Human Brain Responses in Space and Time. *Neuron*. https://doi.org/10.1016/j.neuron.2020.07.001

Cichy, R. M., Pantazis, D., & Oliva, A. (2014). Resolving human object recognition in space and time. *Nature Neuroscience*, *17*(3), 455–462. https://doi.org/10.1038/nn.3635

Davis, J. P., Lander, K., Evans, R., & Jansari, A. (2016). Investigating Predictors of Superior Face Recognition Ability in Police Super-recognisers: Superior face recognisers. *Applied Cognitive Psychology*, *30*(6), 827–840. https://doi.org/10.1002/acp.3260

Duchaine, B. C., Yovel, G., Butterworth, E. J., & Nakayama, K. (2006). Prosopagnosia as an impairment to face-specific mechanisms: Elimination of the alternative hypotheses in a developmental case. *Cognitive Neuropsychology*, *23*(5), 714–747. https://doi.org/10.1080/02643290500441296

Duchaine, B., Germine, L., & Nakayama, K. (2007). Family resemblance: ten family members with prosopagnosia and within-class object agnosia. *Cognitive Neuropsychology*, *24*(4), 419–430. https://doi.org/10.1080/02643290701380491

Duchaine, B., & Nakayama, K. (2006). The Cambridge Face Memory Test: Results for neurologically intact individuals and an investigation of its validity using inverted face stimuli and …. *Neuropsychologia*. https://www.sciencedirect.com/science/article/pii/S0028393205002496

Duchaine, B., & Yovel, G. (2015). A Revised Neural Framework for Face Processing. *Annual Review of Vision Science*, *1*, 393–416. https://doi.org/10.1146/annurev-vision-082114-035518

Dwivedi, K., Bonner, M. F., Cichy, R. M., & Roig, G. (2021). Unveiling functions of the visual

cortex using task-specific deep neural networks. *PLoS Computational Biology*, *17*(8), e1009267. https://doi.org/10.1371/journal.pcbi.1009267

Eimer, M., Gosling, A., & Duchaine, B. (2012). Electrophysiological markers of covert face recognition in developmental prosopagnosia. *Brain: A Journal of Neurology*, *135*(Pt 2), 542–554. https://doi.org/10.1093/brain/awr347

Faghel-Soubeyrand, S., Alink, A., Bamps, E., Gervais, R.-M., Gosselin, F., & Charest, I. (2019). The two-faces of recognition ability: better face recognizers extract different physical content from left and right sides of face stimuli. *Journal of Vision*, *19*(10), 136d – 136d. https://doi.org/10.1167/19.10.136d

Fernandino, L., Tong, J.-Q., Conant, L. L., Humphries, C. J., & Binder, J. R. (2022). Decoding the information structure underlying the neural representation of concepts. *Proceedings of the National Academy of Sciences of the United States of America*, *119*(6). https://doi.org/10.1073/pnas.2108091119

Furl, N., Garrido, L., Dolan, R. J., Driver, J., & Duchaine, B. (2011). Fusiform gyrus face selectivity relates to individual differences in facial recognition ability. *Journal of Cognitive Neuroscience*, *23*(7), 1723–1740. https://doi.org/10.1162/jocn.2010.21545

Fysh, M. C., Stacchi, L., & Ramon, M. (2020). Differences between and within individuals, and subprocesses of face cognition: implications for theory, research and personnel selection. *Royal Society Open Science*, *7*(9), 200233. https://doi.org/10.1098/rsos.200233

Gabay, Y., Dundas, E., Plaut, D., & Behrmann, M. (2017). Atypical perceptual processing of faces in developmental dyslexia. *Brain and Language*, *173*, 41–51. https://doi.org/10.1016/j.bandl.2017.06.004

Garrido, L., Duchaine, B., & DeGutis, J. (2018). Association vs dissociation and setting appropriate criteria for object agnosia [Review of *Association vs dissociation and setting*

appropriate criteria for object agnosia]. *Cognitive Neuropsychology*, *35*(1-2), 55–58. https://doi.org/10.1080/02643294.2018.1431875

Geskin, J., & Behrmann, M. (2018). Congenital prosopagnosia without object agnosia? A literature review. *Cognitive Neuropsychology*, *35*(1-2), 4–54. https://doi.org/10.1080/02643294.2017.1392295

Graumann, M., Ciuffi, C., Dwivedi, K., Roig, G., & Cichy, R. M. (2022). The spatiotemporal neural dynamics of object location representations in the human brain. *Nature Human Behaviour*. https://doi.org/10.1038/s41562-022-01302-0

Grill-Spector, K., Knouf, N., & Kanwisher, N. (2004). The fusiform face area subserves face perception, not generic within-category identification. *Nature Neuroscience*, *7*(5), 555–562. https://doi.org/10.1038/nn1224

Güçlü, U., & van Gerven, M. A. J. (2015). Deep Neural Networks Reveal a Gradient in the Complexity of Neural Representations across the Ventral Stream. *The Journal of Neuroscience: The Official Journal of the Society for Neuroscience*, *35*(27), 10005–10014. https://doi.org/10.1523/JNEUROSCI.5023-14.2015

Harel, A., Kravitz, D., & Baker, C. I. (2013). Beyond perceptual expertise: revisiting the neural substrates of expert object recognition. *Frontiers in Human Neuroscience*, *7*, 885. https://doi.org/10.3389/fnhum.2013.00885

Hebart, M. N., Bankson, B. B., Harel, A., Baker, C. I., & Cichy, R. M. (2018). The representational dynamics of task and object processing in humans. In *eLife* (Vol. 7). https://doi.org/10.7554/elife.32816

Hendel, R. K., Starrfelt, R., & Gerlach, C. (2019). The good, the bad, and the average: Characterizing the relationship between face and object processing across the face recognition spectrum. *Neuropsychologia*, *124*, 274–284.

https://doi.org/10.1016/j.neuropsychologia.2018.11.016

Ince, R. A. A., Giordano, B. L., Kayser, C., Rousselet, G. A., Gross, J., & Schyns, P. G. (2017). A statistical framework for neuroimaging data analysis based on mutual information estimated via a gaussian copula. *Human Brain Mapping*, *38*(3), 1541–1573. https://doi.org/10.1002/hbm.23471

Jiahui, G., Yang, H., & Duchaine, B. (2018). Developmental prosopagnosics have widespread selectivity reductions across category-selective visual cortex. *Proceedings of the National Academy of Sciences of the United States of America*, *115*(28), E6418–E6427. https://doi.org/10.1073/pnas.1802246115

Kaltwasser, L., Hildebrandt, A., Recio, G., Wilhelm, O., & Sommer, W. (2014). Neurocognitive mechanisms of individual differences in face cognition: a replication and extension. *Cognitive, Affective & Behavioral Neuroscience*, *14*(2), 861–878. https://doi.org/10.3758/s13415-013-0234-y

Kaneshiro, B., Perreau Guimaraes, M., Kim, H.-S., Norcia, A. M., & Suppes, P. (2015). A Representational Similarity Analysis of the Dynamics of Object Processing Using Single-Trial EEG Classification. *PloS One*, *10*(8), e0135697. https://doi.org/10.1371/journal.pone.0135697

Kanwisher, N. (2000). Domain specificity in face perception. *Nature Neuroscience*, *3*(8), 759–763. https://doi.org/10.1038/77664

Khaligh-Razavi, S.-M., & Kriegeskorte, N. (2014). Deep supervised, but not unsupervised, models may explain IT cortical representation. *PLoS Computational Biology*, *10*(11), e1003915. https://doi.org/10.1371/journal.pcbi.1003915

Kiani, R., Esteky, H., Mirpour, K., & Tanaka, K. (2007). Object category structure in response patterns of neuronal population in monkey inferior temporal cortex. *Journal of*

Neurophysiology, *97*(6), 4296–4309.

Kriegeskorte, N., & Diedrichsen, J. (2019). Peeling the Onion of Brain Representations. *Annual Review of Neuroscience*, *42*, 407–432. https://doi.org/10.1146/annurev-neuro-080317-061906

Kriegeskorte, N., & Kievit, R. A. (8/2013). Representational geometry: integrating cognition, computation, and the brain. *Trends in Cognitive Sciences*, *17*(8), 401–412.

Kriegeskorte, N., Mur, M., & Bandettini, P. (2008). Representational similarity analysis - connecting the branches of systems neuroscience. *Frontiers in Systems Neuroscience*, *2*, 4. https://doi.org/10.3389/neuro.06.004.2008

Kriegeskorte, N., Mur, M., Ruff, D. A., Kiani, R., Bodurka, J., Esteky, H., Tanaka, K., & Bandettini, P. A. (2008). Matching categorical object representations in inferior temporal cortex of man and monkey. *Neuron*, *60*(6), 1126–1141. https://doi.org/10.1016/j.neuron.2008.10.043

Krizhevsky, A., Sutskever, I., & Hinton, G. E. (2012). ImageNet Classification with Deep Convolutional Neural Networks. In F. Pereira, C. J. C. Burges, L. Bottou, & K. Q. Weinberger (Eds.), *Advances in Neural Information Processing Systems 25* (pp. 1097–1105). Curran Associates, Inc. http://papers.nips.cc/paper/4824-imagenet-classification-with-deep-convolutional-neural-networks.pdf

Lamme, V. A., & Roelfsema, P. R. (2000). The distinct modes of vision offered by feedforward and recurrent processing. *Trends in Neurosciences*, *23*(11), 571–579. https://doi.org/10.1016/s0166-2236(00)01657-x

Langner, O., Dotsch, R., Bijlstra, G., Wigboldus, D. H. J., Hawk, S. T., & van Knippenberg, A. (2010). Presentation and validation of the Radboud Faces Database. *Cognition and*

Emotion, *24*(8), 1377–1388. https://doi.org/10.1080/02699930903485076

Lohse, M., Garrido, L., Driver, J., Dolan, R. J., Duchaine, B. C., & Furl, N. (2016). Effective Connectivity from Early Visual Cortex to Posterior Occipitotemporal Face Areas Supports Face Selectivity and Predicts Developmental Prosopagnosia. *The Journal of Neuroscience: The Official Journal of the Society for Neuroscience*, *36*(13), 3821–3828. https://doi.org/10.1523/JNEUROSCI.3621-15.2016

Long, B., Yu, C.-P., & Konkle, T. (2018). Mid-level visual features underlie the high-level categorical organization of the ventral stream. *Proceedings of the National Academy of Sciences of the United States of America*, *115*(38), E9015–E9024. https://doi.org/10.1073/pnas.1719616115

Maguire, E. A., Valentine, E. R., Wilding, J. M., & Kapur, N. (2003). Routes to remembering: the brains behind superior memory. *Nature Neuroscience*, *6*(1), 90–95. https://doi.org/10.1038/nn988

McDermott, J., Schiller, P. H., & Gallant, J. L. (2002). Spatial frequency and orientation tuning dynamics in area V1. *Proceedings of the*. https://www.pnas.org/content/99/3/1645.short

Murray, E., & Bate, S. (2020). Diagnosing developmental prosopagnosia: repeat assessment using the Cambridge Face Memory Test. *Royal Society Open Science*, *7*(9), 200884. https://doi.org/10.1098/rsos.200884

Naselaris, T., Allen, E., & Kay, K. (2021). Extensive sampling for complete models of individual brains. *Current Opinion in Behavioral Sciences*, *40*, 45–51. https://doi.org/10.1016/j.cobeha.2020.12.008

Noyes, E., Davis, J. P., Petrov, N., Gray, K. L. H., & Ritchie, K. L. (2021). The effect of face masks and sunglasses on identity and expression recognition with super-recognizers and typical observers. *Royal Society Open Science*, *8*(3), 201169.

https://doi.org/10.1098/rsos.201169

Oostenveld, R., Fries, P., Maris, E., & Schoffelen, J.-M. (2011). FieldTrip: Open source software for advanced analysis of MEG, EEG, and invasive electrophysiological data. *Computational Intelligence and Neuroscience*, *2011*, 156869. https://doi.org/10.1155/2011/156869

Popham, S. F., Huth, A. G., Bilenko, N. Y., Deniz, F., Gao, J. S., Nunez-Elizalde, A. O., & Gallant, J. L. (2021). Visual and linguistic semantic representations are aligned at the border of human visual cortex. In *Nature Neuroscience* (Vol. 24, Issue 11, pp. 1628–1636). https://doi.org/10.1038/s41593-021-00921-6

Price, C. J., & Friston, K. J. (2002). Degeneracy and cognitive anatomy. *Trends in Cognitive Sciences*, *6*(10), 416–421. https://doi.org/10.1016/s1364-6613(02)01976-9

Ramon, M. (2021). Super-Recognizers –a novel diagnostic framework, 70 cases, and guidelines for future work. *Neuropsychologia*, 107809. https://doi.org/10.1016/j.neuropsychologia.2021.107809

Rokem, A., & Kay, K. (2020). Fractional ridge regression: a fast, interpretable reparameterization of ridge regression. *GigaScience*, *9*(12). https://doi.org/10.1093/gigascience/giaa133

Rosenthal, G., Tanzer, M., Simony, E., Hasson, U., Behrmann, M., & Avidan, G. (2017). Altered topology of neural circuits in congenital prosopagnosia. *eLife*, *6*. https://doi.org/10.7554/eLife.25069

Rossion, B., & Jacques, C. (2012). The N170: Understanding the time course of face perception in the human brain. *The Oxford Handbook of Event-Related Potential Components.*, *641*, 115–141. https://psycnet.apa.org/fulltext/2013-01016-005.pdf

Russell, R., Duchaine, B., & Nakayama, K. (2009). Super-recognizers: people with

extraordinary face recognition ability. *Psychonomic Bulletin & Review*, *16*(2), 252–257. https://doi.org/10.3758/PBR.16.2.252

Shen, W., Fiori-Duharcourt, N., & Isel, F. (2016). Functional significance of the semantic P600: evidence from the event-related brain potential source localization. *Neuroreport*, *27*(7), 548–558. https://doi.org/10.1097/WNR.0000000000000583

Simonyan, K., & Zisserman, A. (2014). Very Deep Convolutional Networks for Large-Scale Image Recognition. In *arXiv [cs.CV]*. arXiv. http://arxiv.org/abs/1409.1556

Tardif, J., Morin Duchesne, X., Cohan, S., Royer, J., Blais, C., Fiset, D., Duchaine, B., & Gosselin, F. (2019). Use of face information varies systematically from developmental prosopagnosics to super-recognizers. *Psychological Science*, *30*(2), 300–308. https://journals.sagepub.com/doi/abs/10.1177/0956797618811338

Treder, M. S. (2020). MVPA-Light: A Classification and Regression Toolbox for Multi-Dimensional Data. *Frontiers in Neuroscience*, *14*, 289. https://doi.org/10.3389/fnins.2020.00289

van Herten, M., Kolk, H. H. J., & Chwilla, D. J. (2005). An ERP study of P600 effects elicited by semantic anomalies. *Brain Research. Cognitive Brain Research*, *22*(2), 241–255. https://doi.org/10.1016/j.cogbrainres.2004.09.002

Vogel, E. K., McCollough, A. W., & Machizawa, M. G. (2005). Neural measures reveal individual differences in controlling access to working memory. *Nature*, *438*(7067), 500–503. https://doi.org/10.1038/nature04171

Willenbockel, V., Sadr, J., Fiset, D., Horne, G. O., Gosselin, F., & Tanaka, J. W. (2010). Controlling low-level image properties: the SHINE toolbox. *Behavior Research Methods*, *42*(3), 671–684. https://doi.org/10.3758/BRM.42.3.671

Wilmer, J. B., Germine, L., Chabris, C. F., Chatterjee, G., Gerbasi, M., & Nakayama, K. (2012).

Capturing specific abilities as a window into human individuality: the example of face recognition. *Cognitive Neuropsychology*, *29*(5-6), 360–392. https://doi.org/10.1080/02643294.2012.753433

Zadelaar, J. N., Weeda, W. D., Waldorp, L. J., Van Duijvenvoorde, A. C. K., Blankenstein, N. E., & Huizenga, H. M. (2019). Are individual differences quantitative or qualitative? An integrated behavioral and fMRI MIMIC approach. *NeuroImage*, *202*, 116058. https://doi.org/10.1016/j.neuroimage.2019.116058

Supplementary material

Behavioural results

All participants' face recognition ability was assessed using the Cambridge Face Memory Test long-form (CFMT+, (Russell et al. 2009)). Scores on the CFMT+ ranged from 50 to 85 in the typical recognisers group (M_{TRs}=70.00; SD=9.09), and from 92 to 100 in the experimental super-recogniser group (M_{SRs}=95.38, SD=2.68; difference between groups : $t(31)=10.6958$, $p<.00001$ see Fig. 1a). The main experimental task was a one-back task (Fig. 1b). Accuracy was significantly greater for the super-recognisers (M_{SRs}=.93, SD=.054) than for the typical recognisers (M_{TRs}=.83, SD=.094; $t(31)=3.7911$, $p=0.00065$). This was also true when analysing separately face (M_{SRs}= .9260, SD=.0471; M_{TRs}=.8144, SD=.1066; $t(31)=3.8440$, $p=0.00056$) and non-face trials (M_{SRs}=.9456, SD=.0651; M_{TRs}=.8532, SD=.0929; $t(31)=3.2855$, $p=.0025$). Furthermore, accuracy in the one-back task was positively correlated with scores on the CFMT+ ($r=.68$, $p<.001$; RT was marginally associated with CFMT+, $r=.37$, $p=.04$). We observed no significant differences in response times between the two groups ($p>.3$).

Scores obtained by the super-recogniser tested in the UK on a battery of face recognition tests

subject-ID	CFMT+	GFMT	Face Array	LASIE Match	Black and White	Super-rec	Longterm	one-back faces	one-back non-faces
SR-1	93	40	38	83	34	13	9	.9328	0.977
SR-2	95	40	37	88	33	12	9	.8500	0.7903
SR-3	97	40	32	84	33	12	8	.9325	0.9718
SR-4	93	40	38	92	34	13	8	.9726	0.9835
SR-5	98	40	31	91	33	14	9	.9326	0.9787
SR-6	100	40	39	82	40	14	10	.9823	0.9817
SR-7	98	40	40	92	33	13	8	.9319	0.9647
SR-8	96	38	40	90	39	12	10	.9362	0.9787
Max score	102	40	40	100	40	14	10	1	1

Supplementary table 1: The scores above show performance on a battery of standardised face recognition tests (Noyes et al. 2021) for the participants identified as super-recognisers in the UK. Also shown are the scores for our one-back task, for face and non-face trials. The last row of the table shows the maximum obtainable score for each test.

Scores obtained by the super-recogniser tested in Switzerland on a battery of face recognition tests

subject-ID	CFMT+	FICST score	YBT long raw score	one-back faces	one-back non-faces
SR-9	92	0	29	.8132	0.8384
SR-10	99	0	17	.9409	0.9619
SR-11	92	0	20	.9635	0.9808
SR-12	93	1	20	.8581	0.8212
SR-13	92	7	17	.9530	0.985
SR-14	96	0	18	.9604	0.9886
SR-15	94	3	16	.9112	0.9624
SR-16	97	1	22	.9792	0.9643
Best score	102	0	35	1	1

Supplementary table 2: The scores above show performance on a battery of standardised face recognition tests (Ramon, 2021) for the participants identified as super-recognisers in Switzerland. Also shown are the scores for our one-back task, for face and non-face trials. The last row of the table shows the best obtainable score for each test.

Noise ceiling for group-membership decoding using CFMT+ reliability scores

To better interpret the magnitude of our group-membership decoding accuracies, we determined the maximum attainable accuracy when categorising a super-recogniser as such using the CFMT+ (i.e., the empirically imposed noise ceiling for our decoding group-membership analysis). We simulated 1000 distributions of CFMT+ scores, each with N=32, and each having a Pearson correlation of .71±.01 with the distribution of CFMT+ scores observed in this study. The correlation coefficient of .71 was chosen according to the test-retest reliability the CFMT+ measured in previous studies (Arrington et al., 2022; Murray & Bate, 2020). We then predicted super-recogniser participants from these distributions: we compared the simulated SR label (i.e. simulated CFMT+ scores higher than the prescribed cut-off of 92) to the used SR labels. We then averaged the accuracies across the simulated participants, and computed the maximum accuracy from these 1000 distributions. This process was repeated 10000 times, creating a distribution of 10000 simulated maximums with a mean of M=0.9310 (SD=0.0228) that we interpreted as the noise ceiling.

Univariate analyses of EEG associated with individual ability

N170 amplitude and latency. We also performed more traditional event-related potential (ERP) analyses for both groups. We extracted, for face and non-face trials, peak negative ERP

amplitudes and latencies for every participant in a window corresponding to the N170 component (within 110-200 ms at electrodes [B6, B7, B8, A28] on the right hemisphere and [A9, A10, A11, A15] on the left hemisphere). We tested the conditions, groups, and their interaction effects using an ANOVA on N170 peak latency and amplitude separately. No interaction effects were observed for peak latencies ($F_{interaction}(60,1)=1$, $p=.32$) and amplitudes ($F_{interaction}(60,1)=0.32$, $p>.50$). The peak N170 was earlier ($F_{conditions}(60,1)=5.86$, $p=.0185$) and presented greater amplitudes ($F_{conditions}(60,1)=33.78$, $p<.0001$) for faces compared to non-face objects. Moreover, the peak N170 was earlier ($F_{group}(60,1)=19.23$, $p<.0001$) and presented larger amplitudes ($F_{group}(60,1)=13.75$, $p=.0005$) in super-recognisers than typical recognisers.

Lateralisation. Compared to typical recognisers, super-recognisers showed greater N170 peak amplitudes in the right-hemisphere electrodes for faces (computed as the difference between the right [B6, B7, B8, A28] and left [A9, A10, A11, A15]; $t(30)=-2.8542$, $p=.01$). Moreover, the CFMT+ scores of typical recognisers correlated with right-hemisphere lateralisation of the N170 for faces ($r(16)=-.53$, $p=.0298$). These effects were not significant either for non-face stimuli, or for N170 peak latency.

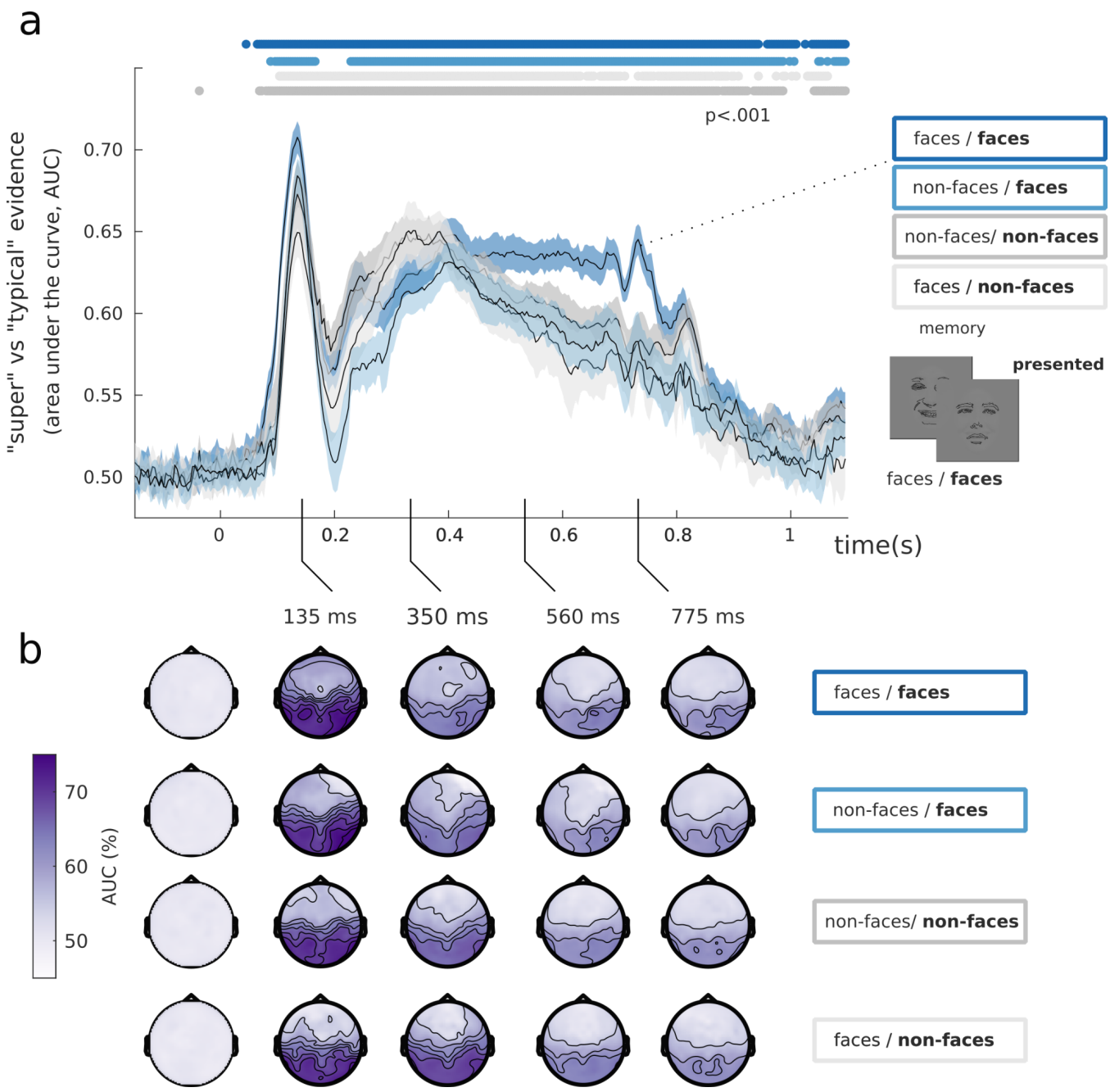

Supplementary figure 1. **a)** We computed the time course of decoding accuracy for group membership from all different face and non-face combinations of one-back and current trials (e.g. consecutive face - face trials). We observed a similar time course for all combinations. However the consecutive face-face trials showed larger decoding accuracies around 400 to 750 ms. **b)** The topographies show results from a searchlight decoding analysis with classification performance attaining 75% accuracy around 135 ms over occipito-temporal electrodes for face presented conditions (74.6% for face-face, 75.1% for nonface-face) and 72% for non-face presented conditions (71.7% for nonface-nonface, 71.5% for face-non-face). Note that drawings of faces are depicted here as an anonymised substitute to the experimental face stimuli presented to our participants.

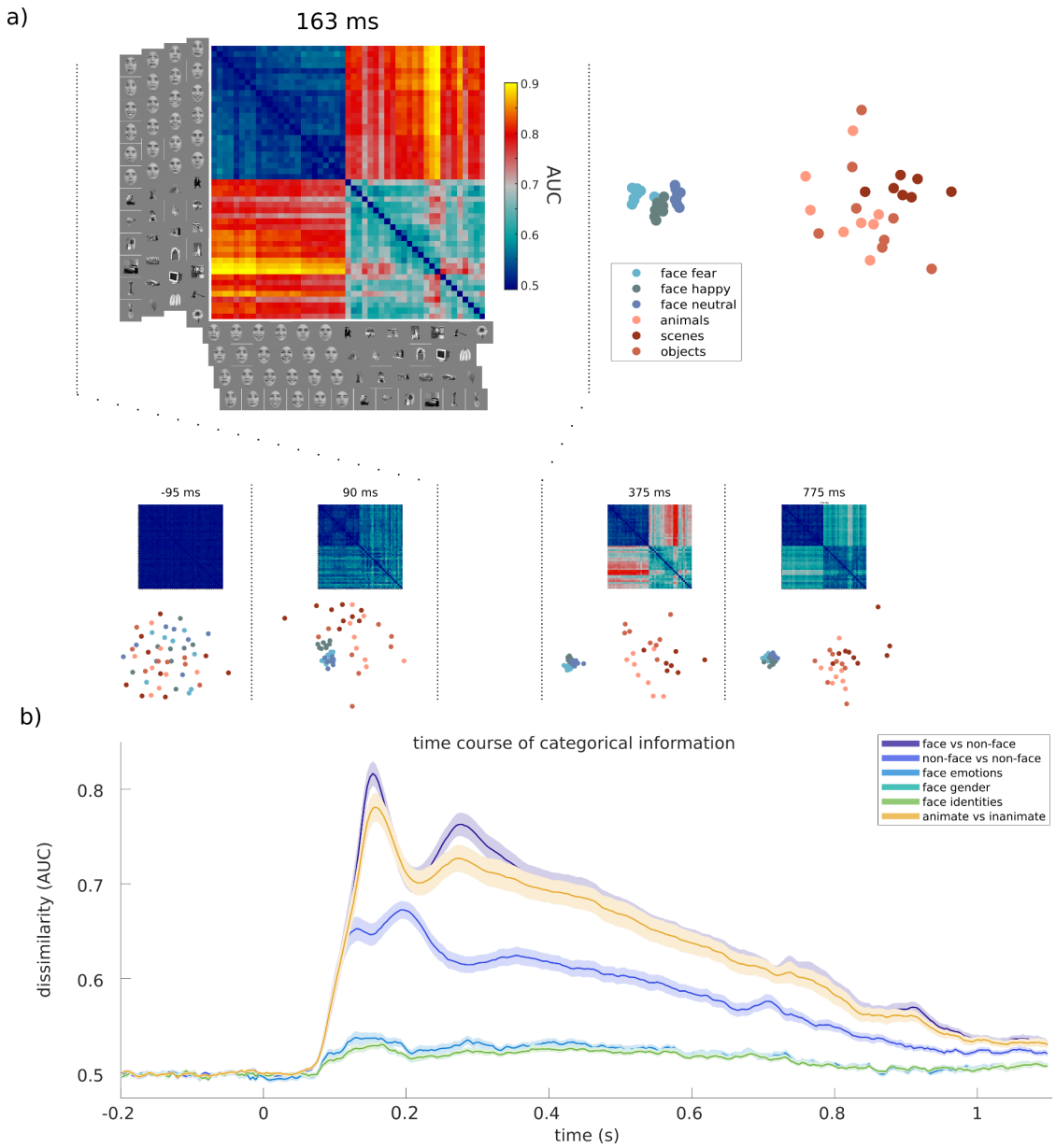

Supplementary figure 2. EEG representational geometry dynamics. a) Representational Similarity Analysis (RSA) was applied to time-resolved EEG patterns, using decoding AUC as dissimilarity measure between pairs of images (5 fold cross-validation, 5 repetitions) to create Representational Dissimilarity Matrices (RDMs). Multidimensional scaling was employed to visualise these high-dimensional brain representations on a 2D plane, which showed clear distinctions between various categories (e.g. face clusters, scenes clusters, animal clusters, etc.). b) We revealed categorical information unfolding in time by averaging dissimilarities between stimulus categories (e.g. faces vs non-face objects) and averaging across participants. Brain representations for the distinction of face vs. non-face objects (a hallmark of

the N170, (Rossion & Jacques, 2012)) dominated all other categorical distinctions (Carlson et al., 2013; Kaneshiro et al., 2015), and peaked at 153 ms.

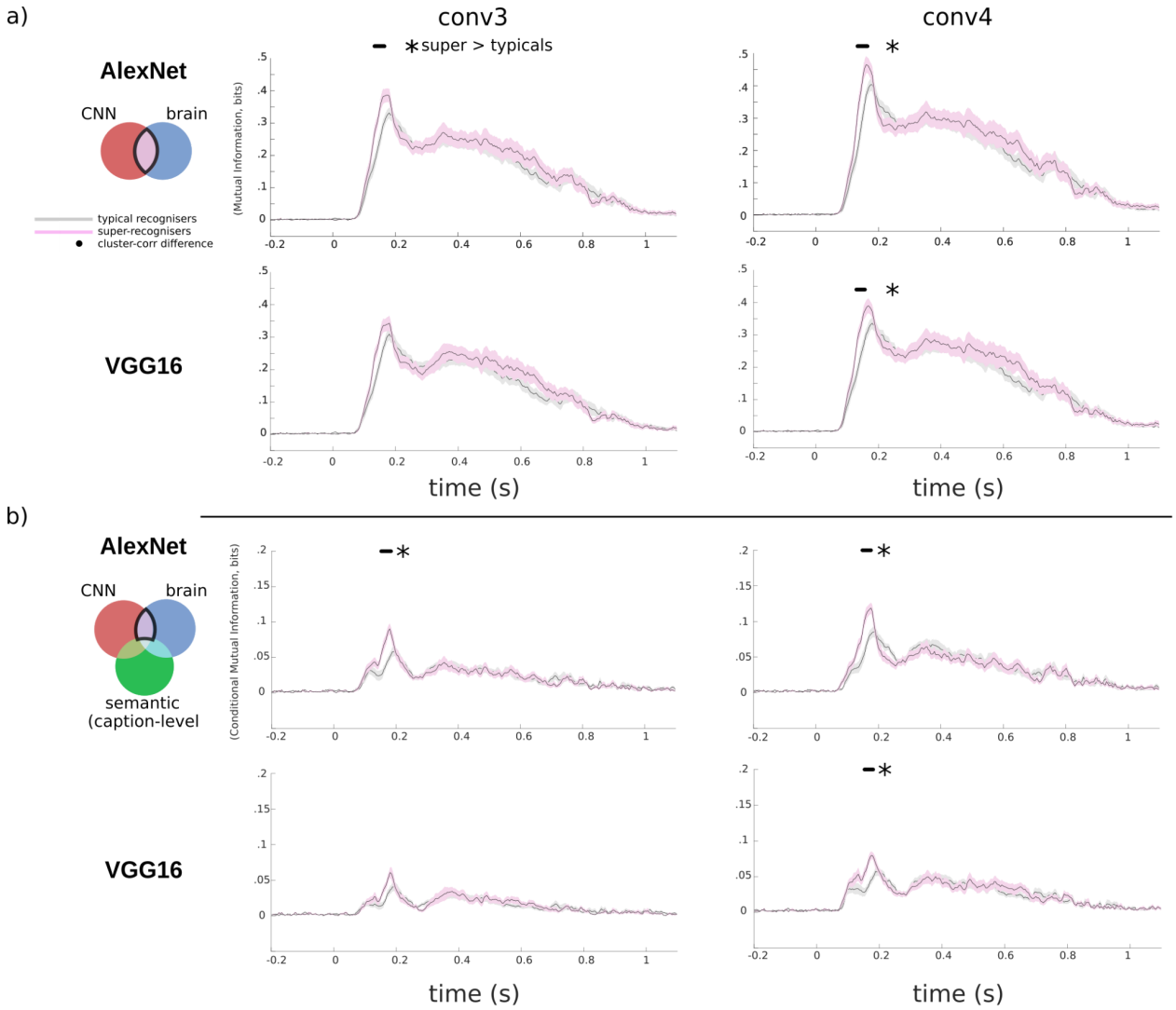

Supplementary figure 3. Comparison of super- and typical-recogniser brain representations with those of artificial neural networks of vision. a) Mutual information results comparing brain RDMs and AlexNet RDMs (first row) and brain RDMs and VGG16 RDMs (second row) are shown for typical- (grey curve) and super-recognisers (pink curve). We found greater similarity with mid-level visual computations as indexed from both CNN models (layers 3, 4 shown for AlexNet and VGG 16) in the brains of super-recognisers (black line indicates significant contrasts, $p<.05$, cluster-corrected) between 130 ms to 160 ms. **b**) We also computed the MI between CNN RDMs and the brain RDMs, but constrained on the Mutual Information from the caption-level semantic RDM. Again, we found greater similarity with mid-level visual computations as indexed from both CNN models (layers 3, 4 shown for AlexNet and VGG 16) in the brains of super-recognisers ($p<.05$, cluster-corrected) between 133 ms to 165 ms. The observed magnitudes were reduced as expected given the additional constraints. The shaded areas of all curves represent the standard error.